Inorg. Chem. **2004**, *43*, 5294–5301

Nitric Oxide Reactivity of Fluorophore Coordinated Carboxylate-Bridged Diiron(II) and Dicobalt(II) Complexes

Scott A. Hilderbrand and Stephen J. Lippard*

Department of Chemistry, Massachusetts Institute of Technology, Cambridge, Massachusetts 02139

Received March 16, 2004

The synthesis, structural characterization, and NO reactivity of carboxylate-bridged dimetallic complexes were investigated. The diiron(II) complex $[Fe_2(\mu\text{-}O_2CAr^{Tol})_4(Ds\text{-}pip)_2]$ (**1**), where O_2CAr^{Tol} = 2,6-di(*p*-tolyl)benzoate and Ds-pip = dansyl-piperazine, was prepared and determined by X-ray crystallography to have a paddlewheel geometry. This complex reacts with NO within 1 min with a concomitant 4-fold increase in fluorescence emission intensity ascribed to displacement of Ds-pip. Although the diiron complex reacts with NO, as revealed by infrared spectroscopic studies, its sensitivity to dioxygen renders it unsuitable as an atmospheric NO sensor. The air-stable dicobalt(II) analogue was also synthesized and its reactivity investigated. In solution, the dicobalt(II) complex exists as an equilibrium between paddlewheel $[Co_2(\mu\text{-}O_2CAr^{Tol})_4(Ds\text{-}pip)_2]$ (**2**) and windmill $[Co_2(\mu\text{-}O_2CAr^{Tol})_2(O_2CAr^{Tol})_2(Ds\text{-}pip)_2]$ (**3**) geometric isomers. Conditions for crystallizing pure samples of each of these isomers are described. Reaction of **2** with excess NO proceeds by reductive nitrosylation giving $[Co(\mu\text{-}O_2CAr^{Tol})_2(NO)_4]$ (**5**), which is accompanied by release of the Ds-pip fluorophore that is *N*-nitrosated in the process. This reaction affords an overall 9.6-fold increase in fluorescence emission intensity, further demonstrating the potential utility of ligand dissociation as a strategy for designing fluorescence-based sensors to detect nitric oxide in a variety of contexts.

Introduction

Our laboratory has recently initiated a program to develop fluorescence-based detection systems for nitric oxide (NO). A review of current strategies for imaging NO[1] highlights our approach, which is to couple transition metal−nitrosyl chemistry with fluorescence signaling. The use of transition metal−nitrosyl forming reactions may ultimately allow for direct detection of NO in biological systems. Our strategy is based on reversing the fluorescence-quenching properties of transition metals that have partially filled d-shells.[2,3] By reaction of NO with a transition metal complex containing a coordinated fluorophore in such a manner as to dissociate the latter from the coordination sphere of the metal, fluorophore emission initially quenched by metal coordination can be restored.

The dioxygen reactivity of carboxylate-bridged non-heme diiron complexes is well-known in biology and has been a focus of research in our laboratory for several years.[4−7] Non-heme diiron enzymes such as hemerythrin, the hydroxylase component of soluble methane monooxygenase, and the R2 component of class I ribonucleotide reductase all react with dioxygen.[4,6,8−10] The NO reactivity of these proteins, which may include ligand dissociation, has also been demonstrated.[11−13] In addition, a synthetic non-heme carboxylate-bridged diiron complex previously prepared by us reacts with NO to form a nitrosyl species.[14] As a result of

* To whom correspondence should be addressed. E-mail: lippard@lippard.mit.edu.

(1) Nagano, T.; Yoshimura, T. *Chem. Rev.* **2002**, *102*, 1235−1269.
(2) Franz, K. J.; Singh, N.; Spingler, B.; Lippard, S. J. *Inorg. Chem.* **2000**, *39*, 4081−4092.
(3) Franz, K. J.; Singh, N.; Lippard, S. J. *Angew. Chem., Int. Ed.* **2000**, *39*, 2120−2122.
(4) Valentine, A. M.; Lippard, S. J. *J. Chem. Soc., Dalton Trans.* **1997**, 3925−3931.
(5) Yoon, S.; Lippard, S. J. *Inorg. Chem.* **2003**, *42*, 8606−8608.
(6) Merkx, M.; Kopp, D. A.; Sazinsky, M. H.; Blazyk, J. L.; Müller, J.; Lippard, S. J. *Angew. Chem., Int. Ed.* **2001**, *40*, 2782−2807.
(7) Lee, D.; Lippard, S. J. *J. Am. Chem. Soc.* **2001**, *123*, 4611−4612.
(8) Stubbe, J.; van der Donk, W. A. *Chem. Rev.* **1998**, *98*, 705−762.
(9) Stenkamp, R. E. *Chem. Rev.* **1994**, *94*, 715−726.
(10) Logan, D. T.; Su, X.-D.; Åberg, A.; Regnström, K.; Hajdu, J.; Eklund, H.; Nordlund, P. *Structure* **1996**, *4*, 1053−1064.
(11) Coufal, D. E.; Tavares, P.; Pereira, A. S.; Hyunh, B. H.; Lippard, S. J. *Biochemistry* **1999**, *38*, 4504−4513.
(12) Haskin, C. J.; Ravi, N.; Lynch, J. B.; Münck, E.; Que, L., Jr. *Biochemistry* **1995**, *34*, 11090−11098.
(13) Nocek, J. M.; Kurtz, D. M., Jr.; Sage, J. T.; Xia, Y.-M.; Debrunner, P.; Shiemke, A. K.; Sanders-Loehr, J.; Loehr, T. M. *Biochemistry* **1988**, *27*, 1014−1024.
(14) Feig, A. L.; Bautista, M. T.; Lippard, S. J. *Inorg. Chem.* **1996**, *35*, 6892−6898.

10.1021/ic049649l CCC: $27.50
Published on Web 07/29/2004

this documented NO reactivity, an investigation was undertaken into the use of carboxylate-bridged dinuclear complexes as potential NO sensors. Although the dioxygen reactivity of diiron complexes with the general formula $[Fe_2(O_2CAr^{Tol})_4(L)_2]$, where O_2CAr^{Tol} = 2,6-di(*p*-tolyl)-benzoate and L = a nitrogen base, has been investigated extensively, their NO chemistry has not.[5,7,15] To examine the potential suitability of these systems for use as NO sensors, related diiron and dicobalt complexes were prepared in which the nitrogen bases were modified to carry a dansyl fluorophore. The synthesis and investigation of the NO reactivity of these complexes is the subject of the present report. This work, along with other previously investigated transition metal fluorescence-based NO detection systems,[2,3,16] contributes to the growing body of evidence supporting ligand dissociation as a general strategy for development of fluorescence-based nitric oxide sensors that evoke an increase in fluorescence intensity upon analyte binding. Some interesting new cobalt chemistry was also discovered during the course of our studies.

Experimental Section

General Considerations. Pentane, tetrahydrofuran (THF), diethyl ether (Et_2O), acetonitrile (CH_3CN), and methylene chloride (CH_2Cl_2) were purified by passage through alumina columns under a N_2 atmosphere.[17] All other solvents were purchased from Mallinckrodt or EM Science and used without further purification. Silica gel 60 (230−400 mesh, EM Science) was used for column chromatography. The starting materials dansyl-piperazine (Ds-pip), HO_2CAr^{Tol}, and $[Fe_2(\mu\text{-}O_2CAr^{Tol})_2(O_2CAr^{Tol})_2(THF)_2]$ were prepared as previously described.[15,18−21] Nitric oxide (Matheson 99%) was purified by a method adapted from the literature.[22] The NO stream was passed through an Ascarite (NaOH fused on silica gel) column and a 6 ft coil filled with silica gel cooled to −78 °C. For fluorescence experiments, NO was introduced into the headspace above the sample solution in a sealed fluorescence cell via a Schlenk manifold. All other reagents were obtained commercially and used without further purification. IR spectra were recorded on a ThermoNicolet Avatar 360 spectrophotometer. In situ IR spectra were recorded on a ReactIR 1000 instrument from ASI equipped with a 1-in.-diameter, 30-reflection silicon ATR (SiComp) probe. UV−vis spectra were recorded on a Hewlett-Packard 8435 spectrophotometer. Unless otherwise mentioned, fluorescence emission intensity spectra were recorded at 25 ± 0.2 °C on a Hitachi F-3010 fluorescence spectrophotometer. Electrospray ionization (ESI) mass spectrometry was performed in the MIT Department of Chemistry Instrumentation Facility. NMR spectra were recorded on a Bruker DPX-400 spectrometer at ambient temperature and referenced to internal ^1H and ^{13}C solvent peaks.

$[Fe_2(\mu\text{-}O_2CAr^{Tol})_4(Ds\text{-}pip)_2]$ (1). To $[Fe_2(\mu\text{-}O_2CAr^{Tol})_2(O_2CAr^{Tol})_2(THF)_2]$ (100 mg, 0.068 mmol) in 10 mL of CH_2Cl_2 was added Ds-pip (44 mg, 0.12 mmol) in 2 mL of CH_2Cl_2, and the resulting solution was allowed to stir under a N_2 atmosphere for 1 h. X-ray quality crystals of **1** (92 mg, 68%) were isolated by vapor diffusion (Et_2O/CH_2Cl_2). IR (KBr, cm^{-1}): 3440 (w br), 3252 (w), 3048 (w), 3018 (w), 2983 (w), 2940 (w), 2918 (w), 2862 (w), 2786 (w), 1605 (s), 1513 (m), 1448 (m), 1403 (s), 1383 (s), 1345 (s), 1330 (m), 1304 (w), 1262 (w), 1229 (w), 1165 (s), 1146 (m), 1063 (w), 933 (m), 842 (w), 813 (m sh), 790 (s), 705 (m), 617 (w), 584 (w), 568 (m), 526 (m), 487 (w), 461 (w). Anal. Calcd for $C_{116}H_{110}N_6O_{12}S_2Fe_2$: C, 71.23; H, 5.67; N, 4.30. Found: C, 70.98; H, 5.77; N, 4.12.

$[Co_2(\mu\text{-}O_2CAr^{Tol})_4(Ds\text{-}pip)_2]$ (2) and $[Co_2(\mu\text{-}O_2CAr^{Tol})_2(O_2CAr^{Tol})_2(Ds\text{-}pip)_2]$ (3). Portions of TEA (460 μL, 3.0 mmol), HO_2CAr^{Tol} (905 mg, 3.0 mmol), $Co(NO_3)_2{\cdot}6(H_2O)$ (455 mg, 1.55 mmol), and Ds-pip (500 mg, 1.55 mmol) were allowed to stir in 75 mL of dry THF for 2.5 h. After removal of the solvent under reduced pressure, the crude residue was extracted with CH_2Cl_2 and filtered through a glass frit of medium porosity. Using approximately one-half of the crude reaction residue, light blue X-ray quality crystals of **2** (400 mg) were prepared by vapor diffusion (Et_2O/CH_2Cl_2) at room temperature. With the remainder of the reaction residue, dark purple X-ray quality crystals of **3** (358 mg) were obtained by vapor diffusion (Et_2O/CH_2Cl_2) at −24 °C. The overall yield of **2** and **3** was 50%.

Characterization of 2. IR (KBr, cm^{-1}): 3247 (w), 3049 (w), 3019 (w), 2985 (w), 2939 (w), 2919 (w), 2862 (w), 2785 (w), 1616 (s), 1585 (m), 1573 (m), 1547 (w sh), 1513 (m), 1449 (m), 1403 (m), 1384 (s), 1344 (m), 1329 (m), 1308 (w), 1261 (w), 1229 (w), 1165 (m), 1147 (m), 1108 (w), 1063 (w), 1023 (w), 937 (m), 844 (w), 813 (m sh), 790 (m), 707 (m), 617 (w), 584 (w), 568 (m), 526 (m), 487 (w), 462 (w). Anal. Calcd for $C_{116}H_{110}N_6O_{12}S_2Co_2$: C, 71.01; H, 5.65; N, 4.28. Found: C, 70.86; H, 5.56; N, 4.30.

Characterization of 3. IR (KBr cm^{-1}): 3252 (w), 3056 (w), 2978 (w), 2942 (w), 2917 (w), 2866 (w), 2791 (w), 1611 (s), 1587 (m sh), 1574 (m sh), 1514 (m), 1454 (m), 1405 (w), 1384 (m), 1345 (m), 1330 (w), 1308 (w), 1260 (w), 1166 (m), 1146 (w), 1112 (w), 1095 (w), 1066 (w), 1048 (w), 1022 (w), 933 (m), 924 (m sh), 851 (w), 822 (m), 801 (s), 781 (m), 763 (w), 735 (w), 714 (m), 616 (w), 584 (w), 566 (m), 544 (w), 521 (w), 487 (w), 468 (w). Anal. Calcd for $C_{116}H_{110}N_6O_{12}S_2Co_2$: C, 71.01; H, 5.65; N, 4.28. Found: C, 70.90; H, 5.83; N, 4.51.

***N*-Nitroso-dansyl-piperazine (4) and $[Co_2(NO)_2(\mu\text{-}O_2CAr^{Tol})_2]$ (5).** Under an atmosphere of Ar, a solution of **2** (120 mg, 0.064 mmol) in 25 mL of CH_2Cl_2 was exposed to excess NO. During the reaction the solution changed color from blue-purple to brown. The solvent was removed in vacuo after stirring under an NO atmosphere for 3 h. The crude residue was washed with 20 mL of Et_2O and filtered, leaving pure **4** (37 mg, 84%) as an off-white solid and a brown Et_2O solution. X-ray quality crystals of **4** were prepared by vapor diffusion (Et_2O/CH_2Cl_2). The brown Et_2O solution was concentrated to 4 mL in vacuo. Dark brown crystals of **5** (34 mg, 63%) were grown from the concentrated Et_2O solution at −40 °C. It was also possible to isolate the free carboxylic acid, HO_2CAr^{Tol} (**6**), from the remaining Et_2O mother liquor; however, no attempt was made to obtain a yield.

Characterization of 4. ^1H NMR (400 MHz, CD_2Cl_2): δ 8.59 (1 H, d, J = 7.6 Hz), 8.31 (1 H, d, J = 8.7 Hz), 8.20 (1 H, dd, J = 7.4, 1.3 Hz), 7.59−7.54 (2 H, m), 7.20 (1 H, d, J = 7.1 Hz), 4.28 (2 H, t, J = 5.2 Hz), 3.82 (2 H, t, J = 5.4 Hz), 3.43 (2 H, t, J = 5.3 Hz), 3.17 (2 H, t, J = 5.3 Hz), 2.87 (6 H, s). ^{13}C NMR (100 MHz, CD_2Cl_2): δ 152.61, 132.77, 131.78, 131.33, 130.64, 128.90, 123.72, 119.43, 115.56, 49.66, 46.59, 45.71, 45.12, 39.28. IR (KBr, cm^{-1}): 2980 (w), 2939 (w), 2864 (w), 2786 (w), 1588

(15) Lee, D.; Lippard, S. J. *Inorg. Chem.* **2002**, *41*, 2704−2719.
(16) Hilderbrand, S. A.; Lim, M. H.; Lippard, S. J. *J. Am. Chem. Soc.* **2004**, *126*, 4972−4978.
(17) Pangborn, A. B.; Giardello, M. A.; Grubbs, R. H.; Rosen, R. K.; Timmers, F. J. *Organometallics* **1996**, *15*, 1518−1520.
(18) Saavedra, J. E.; Booth, M. N.; Hrabie, J. A.; Davies, K. M.; Keefer, L. K. *J. Org. Chem.* **1999**, *64*, 5124−5131.
(19) Du, C.-J. F.; Hart, H.; Ng, K.-K. D. *J. Org. Chem.* **1986**, *51*, 3162−3165.
(20) Saednya, A.; Hart, H. *Synthesis* **1996**, 1455−1458.
(21) Chen, C.-T.; Siegel, J. S. *J. Am. Chem. Soc.* **1994**, *116*, 5959−5960.
(22) Lorković, I. M.; Ford, P. C. *Inorg. Chem.* **2000**, *39*, 632−633.

(w), 1573 (w), 1502 (w), 1485 (w), 1454 (m), 1429 (m), 1404 (w), 1357 (m), 1336 (s), 1319 (m), 1284 (m), 1227 (m), 1198 (w), 1162 (s), 1109 (m), 1075 (w), 1057 (w), 1045 (w), 987 (m), 924 (s), 810 (w), 793 (s), 773 (w), 713 (s), 682 (w), 622 (m), 602 (m), 570 (m), 538 (w), 485 (w), 474 (m). MS-ESI (*m*/*z*): $[M + Na]^+$ Calcd for $NaC_{16}H_{20}N_4O_3S$, 371.1154. Found 371.1133.

Characterization of 5. IR (KBr, cm^{-1}): 3049 (w), 3023 (w), 2918 (w), 2861 (w), 1861 (m), 1785 (s), 1754 (s), 1588 (s), 1561 (s), 1515 (m), 1447 (m), 1406 (m), 1388 (m), 1109 (w), 847 (w), 815 (m), 790 (m), 762 (w), 728 (w), 715 (w), 703 (w), 586 (w), 540 (w), 525 (m). Anal. Calcd for $C_{42}H_{34}N_4O_8Co_2$: C, 60.01; H, 4.08; N, 6.66. Found: C, 60.17; H, 4.27; N, 6.44.

X-ray Crystallography. Single crystals suitable for data collection were covered in Infineum V8512 (formerly called Paratone N oil) mounted on the tips of quartz capillary tubes and transferred to the −100 °C low-temperature nitrogen stream a Bruker KRYOFLEX BVT-AXS cryostat. Data were collected on the Bruker diffractometer (Mo Kα $\lambda = 0.71073$ Å) controlled by the SMART software package running on a Pentium II PC.[23] The general procedures used for data collection are reported elsewhere.[24] Empirical absorption corrections were calculated with the SADABS program.[25] Structures were solved and refined with the SHELXTL and SAINTPLUS software packages on a Pentium II PC running the Windows NT operating system.[26,27] All non-hydrogen atoms were refined anisotropically by least-squares cycles and Fourier syntheses. Hydrogen atoms were assigned idealized positions and given thermal parameters of 1.2 times the thermal parameter of the carbon or nitrogen atom to which each was attached. All structure solutions were checked for higher symmetry with the PLATON program.[28]

Two of the CH_2Cl_2 molecules in the structure of **1** are disordered. In the first disordered CH_2Cl_2, one of the chlorine atoms resides in two positions and was refined with 50% occupancy for each atom. The second CH_2Cl_2 molecule also has a disordered chlorine atom that was modeled with 75% and 25% occupancies. In the structure of **2**, three of the CH_2Cl_2 solvent molecules are disordered. The first has a chlorine atom disordered over two positions with 60% and 40% occupancies. The remaining two disordered CH_2Cl_2 atoms in **2** are each disordered over two positions, both with 100% occupancy of the central carbon atom. The chlorine atoms are disordered over two sites modeled with 60% and 40% occupancies for the first solvent molecule and 75% and 25% for the second. The oxygen atom of the nitrosyl group in **4** is disordered over two positions and was refined with occupancies of 55% and 45%.

Results and Discussion

Synthesis. A range of iron terphenylcarboxylato complexes having a variety of *N*-donor ligands have been prepared and reported in the literature.[5,7,15,29] Complex **1** was synthesized in a similar manner. The reaction of 2 equiv of dansyl-piperazine with $[Fe_2(\mu\text{-}O_2CAr^{Tol})_2(O_2CAr^{Tol})_2(THF)_2]$ under an inert atmosphere in CH_2Cl_2 followed by crystallization from vapor diffusion of Et_2O into the CH_2Cl_2 solution afforded **1** in 68% yield as light yellow-green crystals. The reaction is complete in less than 1 h. The fluorescence emission intensity of crystalline **1** is significantly diminished by comparison to a solid sample of dansyl-piperazine when illuminated with long-wavelength UV light from a hand held lamp. All previously prepared tetra(carboxylato)diiron(II) complexes obtained in our laboratory are sensitive to O_2 and have been used to investigate structural and mechanistic aspects of O_2 binding and activation parallel to that occurring in carboxylate-bridged diiron containing proteins.[15] Given the similarity of **1** to these previously reported diiron complexes, it is not surprising that **1** is sensitive to O_2, both when dissolved in halogenated solvents and in the solid state.

In order to obtain tetracarboxylatodimetal(II) complexes having no O_2 sensitivity, the chemistry of the dicobalt(II) analogue was examined. The related dicobalt(II) complex, $[Co_2(\mu\text{-}O_2CAr^{Tol})_2(O_2CAr^{Tol})_2(C_5H_5N)_2]$, which contains two pyridine ligands, is air stable.[30] There are a few examples of air-stable cobalt(II) complexes, such as $[Co(^iPrDATI)_2]$, that react with NO via a reductive nitrosylation mechanism.[2] The synthesis of the dicobalt(II) analogue of **1** was therefore undertaken. Complex **2** was formed by the reaction of $Co(NO_3)_2{\cdot}6(H_2O)$ with dansyl-piperazine, HO_2CAr^{Tol}, and triethylamine in a 1:1:2:2 ratio in THF. Blue rod-shaped crystals of **2** were isolated by vapor diffusion of Et_2O into a blue-purple solution of the dicobalt complex in CH_2Cl_2 at room temperature. When the crystallization setup was maintained at −24 °C or below, however, **3** was isolated as purple plates. The overall isolated yield for **2** and **3** from the same reaction, under different crystallization conditions optimized for each, was 50%. As with $[Co_2(\mu\text{-}O_2CAr^{Tol})_2(O_2CAr^{Tol})_2(C_5H_5N)_2]$, both **2** and **3** are air stable for an extended period both as solids and in solution, and both can be synthesized on the benchtop. The interconversion of the dicobalt complex between the blue-purple paddlewheel-core and purple windmill-core structures (Scheme 1) is temperature dependent, as discussed in more detail below.

Scheme 1

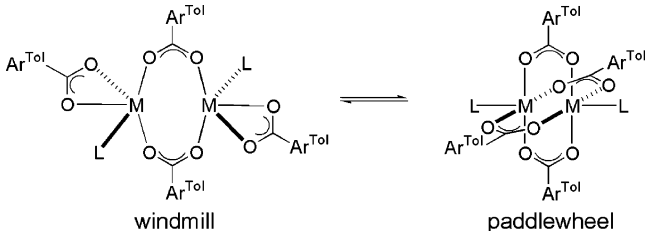

Structural Characterization of the Diiron(II) and Dicobalt(II) Complexes. Crystallographic data and selected geometric information for **1**−**3** are given in Tables 1 and 2, respectively. The structural diagrams are presented Figures 1 and 2. Complex **1** adopts a paddlewheel geometry with four 1,3-bridging carboxylate ligands and two Ds-pip fluo-

(23) *SMART: Software for the CCD Detector System*, version 5.626; Bruker AXS: Madison, WI, 2000.
(24) Kuzelka, J.; Mukhopadhyay, S.; Spingler, B.; Lippard, S. J. *Inorg. Chem.* **2004**, *43*, 1751−1761.
(25) Sheldrick, G. M. *SADABS: Area-Detector Absorption Correction*, version 5.01; University of Göttingen, Göttingen, Germany, 2001.
(26) *SHELXTL: Program Library for Structure Solution and Molecular Graphics*, version 6.2; Bruker AXS: Madison, WI, 2001.
(27) *SAINTPLUS: Software for the CCD Detector System*, version 6.1; Bruker AXS: Madison, WI, 2001.
(28) Spek, A. L. *PLATON, A Multipurpose Crystallographic Tool*; Utrecht University: Utrecht, The Netherlands, 2000.
(29) Chavez, F. A.; Ho, R. Y. N.; Pink, M.; Young, V. G., Jr.; Kryatov, S. V.; Rybak-Akimova, E. V.; Andres, H.; Münck, E.; Que, L., Jr.; Tolman, W. B. *Angew. Chem., Int. Ed.* **2002**, *41*, 149−152.
(30) Lee, D.; Hung, P.-L.; Spingler, B.; Lippard, S. J. *Inorg. Chem.* **2002**, *41*, 521−531.

Table 1. Summary of X-ray Crystallographic Information for Compounds **1**−**5**

	1·4CH_2Cl_2	**2**·4CH_2Cl_2	**3**·Et_2O	**4**	**5**·CH_2Cl_2
formula	$C_{120}H_{118}O_{12}N_6S_2Cl_8Fe_2$	$C_{120}H_{118}O_{12}N_6S_2Cl_8Co_2$	$C_{120}H_{120}O_{13}N_6S_2Co_2$	$C_{16}H_{20}O_3N_4S$	$C_{43}H_{36}O_8N_4Cl_2Co_2$
fw	2295.70	2301.79	2036.27	348.42	925.54
space group	$P\bar{1}$	$P\bar{1}$	$P\bar{1}$	$C2/c$	$P\bar{1}$
a, Å	15.219(3)	15.191(7)	12.582(3)	28.32(1)	11.983(2)
b, Å	19.752(4)	19.660(9)	13.760(4)	6.594(3)	12.907(2)
c, Å	21.337(4)	21.30(1)	16.521(3)	19.966(9)	14.474(2)
α, deg	116.18(3)	115.974(7)	100.98(1)		71.121(2)
β, deg	105.44(3)	105.37(1)	106.60(1)	117.454	76.355(2)
γ, deg	90.63(3)	90.353(8)	103.58(2)		77.119(2)
V, Å^3	5487(1)	5459(5)	2560(1)	3309(3)	2032.2(5)
Z	2	2	1	8	2
ρ_{calcd}, g/cm^3	1.387	1.379	1.314	1.399	1.432
T, °C	−100	−100	−100	−100	−100
μ(Mo Kα), mm^{-1}	0.562	0.603	0.432	0.219	0.939
total no. of data	47931	48323	22865	14013	17868
no. of unique data	24367	24669	11629	3918	9120
no. of params	1369	1409	655	307	532
R[a] (%)	7.43	6.96	6.73	6.00	4.02
wR^2 [b] (%)	15.80	17.91	16.87	12.15	10.42
max, min peaks, e/Å^3	0.811, −0.744	1.742, −0.954	0.929,−0.317	0.482, −0.283	0.643, −0.438

[a] $R = \sum||F_o| - F_c||/\sum|F_o|$. [b] $wR^2 = \{w(F_o^2 - F_c^2)^2/\sum[w(F_o^2)^2]\}^{1/2}$.

Table 2. Selected Bond Distances and Angles for **1**, **2**, and **3**[a]

distance	(Å)	angle	(deg)
	1		
Fe1−Fe2	2.725(1)	N1−Fe1−Fe2	159.55(9)
Fe1−N1	2.138(3)	N1−Fe1−O1	95.6(1)
Fe1−O1	2.084(3)	N1−Fe1−O3	113.2(2)
Fe1−O3	2.074(3)	N1−Fe1−O5	97.2(1)
Fe1−O5	2.066(2)	N1−Fe1−O7	83.8(1)
Fe1−O7	2.162(3)	N4−Fe2−Fe1	159.54(9)
Fe2−N4	2.122(3)	N4−Fe2−O2	100.6(1)
Fe2−O2	2.052(2)	N4−Fe2−O4	87.5(1)
Fe2−O4	2.126(3)	N4−Fe2−O6	95.8(1)
Fe2−O6	2.064(3)	N4−Fe2−O8	110.9(1)
Fe2−O8	2.042(3)		
	2		
Co1−Co2	2.720(2)	N1−Co1−Co2	163.95(8)
Co1−N1	2.114(3)	N1−Co1−O1	96.2(1)
Co1−O1	2.039(2)	N1−Co1−O3	108.2(1)
Co1−O3	1.993(2)	N1−Co1−O5	98.9(1)
Co1−O5	2.033(2)	N1−Co1−O7	84.7(1)
Co1−O7	2.031(2)	N4−Co2−Co1	164.38(8)
Co2−N4	2.128(3)	N4−Co2−O2	96.7(1)
Co2−O2	2.051(2)	N4−Co2−O4	86.5(1)
Co2−O4	2.038(2)	N4−Co2−O6	96.0(1)
Co2−O6	2.066(2)	N4−Co2−O8	109.9(1)
Co2−O8	2.024(3)		
	3		
Co1−Co1A	3.898(1)	O1−Co1−N1	101.0(1)
Co−N1	2.079(3)	O1−Co1−O3	118.0(1)
Co−O1	1.938(2)	O3−Co1−N1	93.8(1)
Co−O3	1.951(3)		

[a] Numbers in parentheses are estimated standard deviations of the last significant figure. Atoms are labeled as indicated in Figures 1 and 2.

rophores occupying apical positions along the Fe−Fe vector. This core is structurally similar to that in several other tetra(μ-carboxylato)diiron(II) complexes previously investigated in our laboratory. The Fe−Fe distance of 2.725(1) Å is significantly shorter than the reported 4.2822(7) Å value in $[Fe_2(\mu\text{-}O_2CAr^{Tol})_2(O_2CAr^{Tol})_2(THF)_2]$, which adopts the more open windmill geometry,[15] but nearly identical to the 2.7277(7) Å distance in the paddlewheel isomer of $[Fe_2(\mu\text{-}O_2CAr^{4-FPh})_4(THF)_2]$. The Fe−Fe distances of other paddlewheel complexes with nitrogenous bases, such as 1-methylimidazole, pyridine, and 4-*tert*-butylpyridine, coordinated

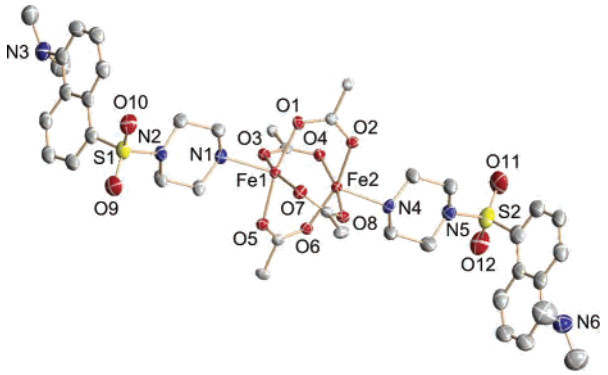

Figure 1. Structural diagram of $[Fe_2(\mu\text{-}O_2CAr^{Tol})_4(Ds\text{-}pip)_2]$ (**1**) showing 50% probability thermal ellipsoids. The *m*-tolyl terphenylcarboxylate ligands have been truncated, and the solvent molecule has been omitted for clarity.

in the axial sites range between 2.823 and 2.848 Å. The shortened Fe−Fe distance in **1** by comparison to these other nitrogen base adducts is not a consequence of steric interactions. Although rather bulky, the Ds-pip ligands in **1** are oriented away from the diiron core, thereby minimizing steric crowding. The average Fe−N bond length in **1** of 2.130(3) Å is somewhat longer than the 2.041−2.098 Å range reported for the structurally characterized complexes having imidazole and pyridine ligands. The longer Fe−N distances in **1** are consistent with expectations based on the diminished π-acceptor ability of the piperazine in comparison to imidazole and pyridine. This feature most likely effects shortening of the Fe−Fe distance.

A carboxylate shift must occur during the reaction of $[Fe_2(\mu\text{-}O_2CAr^{Tol})_2(O_2CAr^{Tol})_2(THF)_2]$ with dansyl-piperazine to form **1**, since the former has a windmill configuration with only two bridging carboxylate ligands. Interconversion between the windmill and paddlewheel geometries can occur by carboxylate shifts of two of the bridging carboxylate ligands in the tetra-bridged paddlewheel structure to give the doubly bridged windmill geometry. The temperature dependence of these carboxylate shifts was previously investigated by ^{19}F NMR spectroscopic analysis of tetra(carboxylato)diiron(II) complexes carrying the fluoro-

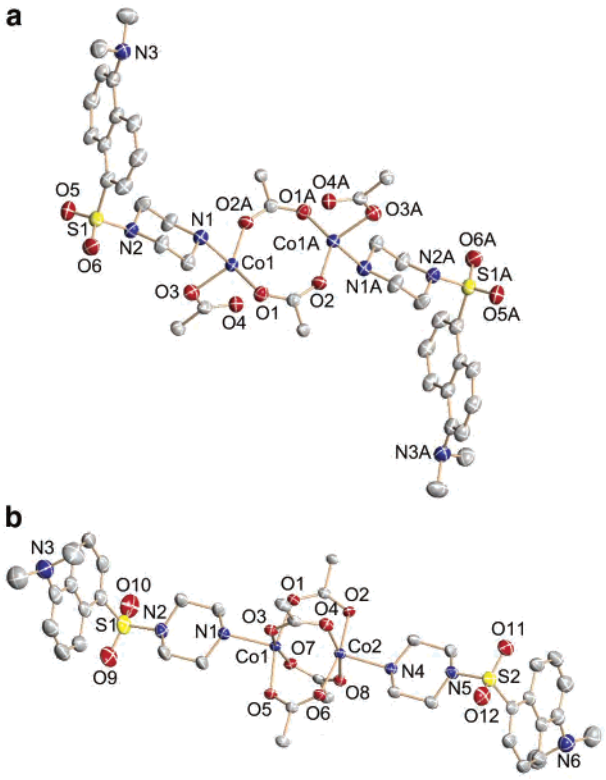

Figure 2. Structural diagrams of (a) $[Co_2(\mu\text{-}O_2CAr^{Tol})_4(Ds\text{-}pip)_2]$ (**2**) and (b) $[Co_2(\mu\text{-}O_2CAr^{Tol})_2(O_2CAr^{Tol})_2(Ds\text{-}pip)_2]$ (**3**) showing 50% probability thermal ellipsoids. The *m*-tolyl terphenylcarboxylate ligands have been truncated, and the solvent molecules have been omitted for clarity.

substituted 2,6-di(4-fluorophenyl)benzoate analogue of the HO_2CAr^{Tol} ligand.[15] Variable temperature ^{19}F NMR spectra of $[Fe_2(\mu\text{-}O_2CAr^{4FPh})_2(O_2CAr^{4-FPh})_2(THF)_2]$ displayed three fluorine resonances that can be attributed to the bridging and terminal carboxylate ligands in the windmill geometry, $[Fe_2(\mu\text{-}O_2CAr^{4-FPh})_2(O_2CAr^{4-FPh})_2(THF)_2]$. Cooling of the sample to below −60 °C gave a single fluorine signal, which can be accounted for by invoking a paddlewheel structure, $[Fe_2(\mu\text{-}O_2CAr^{4FPh})_4(THF)_2]$, where the fluorine substituents of the four bridging carboxylate ligands are in identical magnetic environments.[15]

In an attempt to isolate the corresponding windmill structure of **1**, vapor diffusion crystallization chambers were set-up at multiple temperatures down to −40 °C. Under all conditions investigated, only the paddlewheel complex was isolated. These results are not surprising, however, in view of the variable temperature ^{19}F NMR results for $[Fe_2(\mu\text{-}O_2CAr^{4-FPh})_4(4\text{-}^tBuC_5H_4N)_2]$.[15] Unlike the THF complex, which shows a distinctive temperature dependence of its ^{19}F NMR signals, only a single sharp fluorine resonance is observed with $[Fe_2(\mu\text{-}O_2CAr^{4-FPh})_4(4\text{-}^tBuC_5H_4N)_2]$ between 20 and −70 °C, indicating that the paddlewheel structure is favored over the windmill geometry.[15] Therefore, assuming that the stability of **1** is similar to that of $[Fe_2(\mu\text{-}O_2CAr^{4-FPh})_4(4\text{-}^tBuC_5H_4N)_2]$, it is unlikely that the windmill structure could be isolated.

The geometry of the dicobalt(II) Ds-pip complex, however, is temperature dependent. X-ray diffraction studies of **2** and **3** reveal their respective paddlewheel and windmill structures,

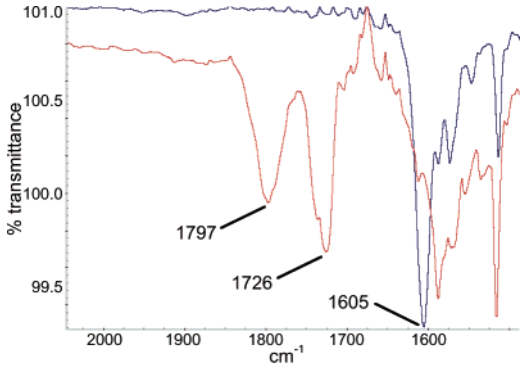

Figure 3. Solution IR traces of $[Fe_2(\mu\text{-}O_2CAr^{Tol})_4(Ds\text{-}pip)_2]$ (**1**) in CH_2Cl_2 before (blue) and 90 min after (red) addition of 10 equiv of NO.

providing the first example of a dicobalt(II) terphenylcarboxylate complex where such isomers have been isolated. In contrast to $[Fe_2(\mu\text{-}O_2CAr^{4-FPh})_4(THF)_2]$, which has the paddlewheel geometry at low temperature,[15] the windmill structure is favored for **3** at −24 °C, as demonstrated by crystallography. The observed difference in relative stability of the windmill and paddlewheel geometries of $[Fe_2(O_2CAr^{4-FPh})_4(THF)_2]$[25] and $[Co_2(\mu\text{-}O_2CAr^{Tol})_4(Ds\text{-}pip)_2]$ at diminished temperature may be a consequence of the slightly different ligand environments and different transition metals used. The carboxylate shift involved in the transition from **2** to **3** results in an increase of the Co−Co distance from 2.720(2) to 3.898(1) Å. The latter distance is in good agreement with the previously reported value of 3.9168(7) Å in $[Co_2(\mu\text{-}O_2CAr^{Tol})_2(O_2CAr^{4-Tol})_2(C_5H_4N)_2]$.[30] The solid-state IR spectra of **2** and **3** are very similar, despite the shift in coordination environment at the two cobalt centers. The carboxylate stretch at 1616 cm^{-1} in **2** shifts to 1611 cm^{-1} in **3**. No additional carboxylate stretching bands are observed in **3**, even though the carboxylate ligands have two different coordination modes. The diiron(II) paddlewheel complex **1** is isomorphous with the corresponding dicobalt(II) complex, with both crystallizing in space group $P\bar{1}$. The distances between the two metal centers are essentially identical, being 2.725(1) and 2.720(2) Å in **1** and **2**, respectively; the average Co−N distance of 2.121(3) Å in **2** is nearly the same as the average value of 2.130(3) Å in **1**.

Reactivity of $[Fe_2(\mu\text{-}O_2CAr^{Tol})_4(Ds\text{-}pip)_2]$ (1). Addition of NO to a solution of **1** in CH_2Cl_2 results in an immediate color change from light yellow-green to brown. Compound **1** is also sensitive toward O_2. When CH_2Cl_2 solutions of **1** are exposed to air at room temperature, a light yellow solution is obtained. Although the O_2 reactivity of **1** was not studied in detail, similar diiron(II) tetracarboxylate complexes have been investigated extensively.[5,7,15,29,31]

The reaction of **1** with NO was monitored by solution IR spectroscopy. When 10 equiv of NO was admitted to a sealed flask containing a 0.5 mM solution of **1** in CH_2Cl_2, new IR bands at 1797 and 1726 cm^{-1} appeared (Figure 3). These features are consistent with formation of an $Fe(NO)_2$ unit. The distinctive carboxylate stretching band of the starting

(31) Costas, M.; Cady, C. W.; Kryatov, S. V.; Ray, M.; Ryan, M. J.; Rybak-Akimova, E. V.; Que, L., Jr. *Inorg. Chem.* **2003**, *42*, 7519−7530.

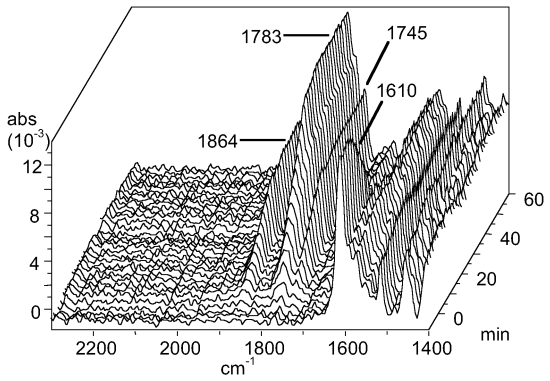

Figure 4. Time dependent solution IR traces of $[Co_2(\mu\text{-}O_2CAr^{Tol})_4(Ds\text{-}pip)_2]$ (**2**) in CH_2Cl_2 after exposure to excess NO over a period of 1 h. Individual spectra were recorded every 60 s.

complex at 1605 cm^{-1} also disappears. These IR data indicate potential disruption of the diiron core in **1**. The possibility exists that a diiron tetranitrosyl complex having two bridging carboxylate ligands may have formed. Such a diiron tetranitrosyl complex could be isostructural to $[Co_2(\mu\text{-}O_2CAr^{Tol})_2(NO)_4]$, vide infra. All attempts to isolate and characterize structurally the iron nitrosyl products from the reaction of **1** with NO proved to be unsuccessful. Several reactions with different amounts of NO ranging from 1 to 200 equiv were investigated. Reaction of **1** with 200 equiv of NO gave a few brown crystals when recrystallized over an atmosphere of excess NO. The brown crystals, formed together with a light tan precipitate, did not diffract X-rays. No further characterization of the crystals was attempted.

Reactivity of the Dicobalt Complexes 2 and 3 with Nitric Oxide. Reactions of the dicobalt terphenylcarboxylate complexes with nitric oxide were performed at room temperature, where **2** is expected to be the predominant species in solution. Since the windmill and paddlewheel isomers are present in equilibrium with each other, it is uncertain which is more reactive with NO. The reaction of **2** with excess NO in CH_2Cl_2 was followed by IR spectroscopy in situ, revealing several new features (Figure 4) as the solution color changed from blue-purple to brown. The most noticeable change was the appearance of peaks at 1864 and 1783 cm^{-1}, which first begin to form 6 min after exposure to NO. These IR bands are consistent with formation of a cobalt(I) dinitrosyl species.[2] In addition, the carboxylate stretching mode at 1610 cm^{-1} in **2** disappeared as the reaction progressed, indicating a significant change in the structure later confirmed by X-ray crystallography, vida infra. A final IR feature at 1745 cm^{-1} appeared as the reaction progressed, consistent with the presence of free carboxylic acid.

Table 3. Selected Bond Distances and Angles for **4** and **5**[a]

distance	(Å)	angle	(deg)
		4	
$N4-O3_{av}$	1.06(4)	$N1-N4-O3_{av}$	126(1)
N1−N4	1.322(3)	N4−N1−C13	121.4(2)
		N4−N1−C14	121.3(2)
		5	
$Co-NO_{av}$	1.662(5)	$Co-N-O_{av}$	163(1)
$N-O_{av}$	1.15(1)	N3−Co1−O1	114.71(8)
Co1−O1	1.982(1)	N3−Co1−O3	120.16(8)
Co1−O3	1.983(1)	N3−Co1−N4	109.8(1)
Co2−O2	1.974(1)	N4−Co1−O1	106.53(8)
Co2−O4	1.978(1)	N4−Co1−O3	110.04(8)
		O1−Co1−O3	94.16(5)
		N1−Co2−O2	110.73(8)
		N1−Co2−O4	106.94(8)
		N1−Co2−N2	110.4(1)
		N2−Co2−O2	116.08(8)
		N2−Co2−O4	117.41(8)
		O2−Co2−O4	94.12(5)

[a] Numbers in parentheses are estimated and calculated standard deviations of the last significant figure for the single and average values, respectively. Atoms are labeled as indicated in Figure 5.

The products from the reaction of **2** with NO in CH_2Cl_2 were isolated and characterized by X-ray crystallography (Scheme 2). Selected bond lengths and structural diagrams of **4** and **5** are given in Table 3 and Figure 5, respectively. After removal of the solvent from the NO reaction, the residue was washed with Et_2O, leaving behind **4** in 84% yield. Light yellow rods of **4**, which fluoresce under UV illumination, were prepared by vapor diffusion of Et_2O into a CH_2Cl_2 solution of the compound. X-ray crystallographic analysis of **4** indicated that the Ds-pip ligands in **2** underwent *N*-nitrosation during the NO reaction. The ^1H NMR spectrum of **4** reveals that the methylene protons of the piperazine

Scheme 2

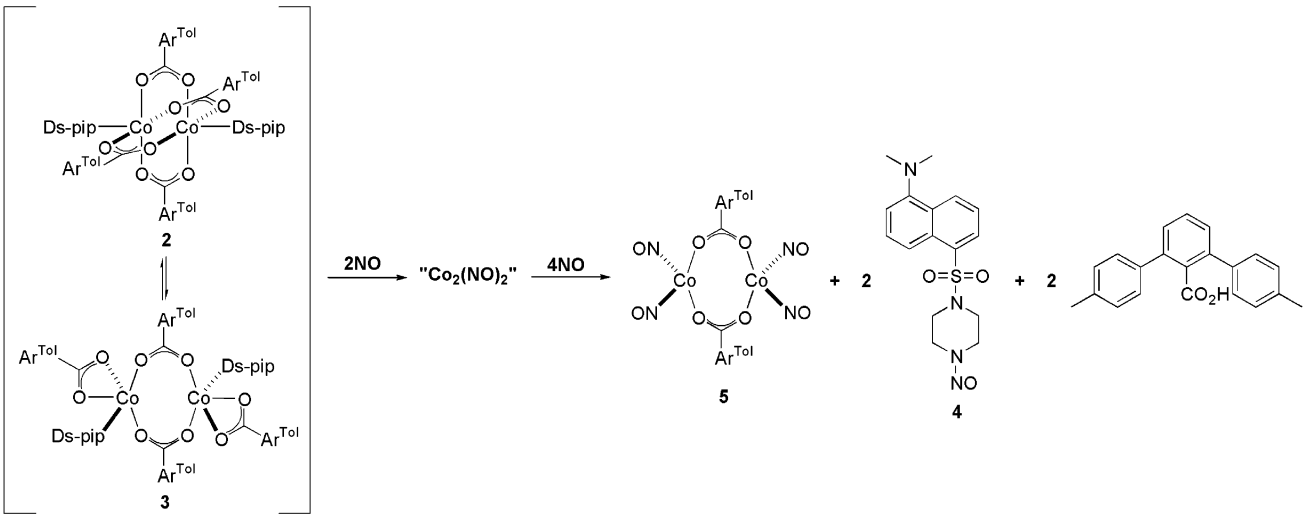

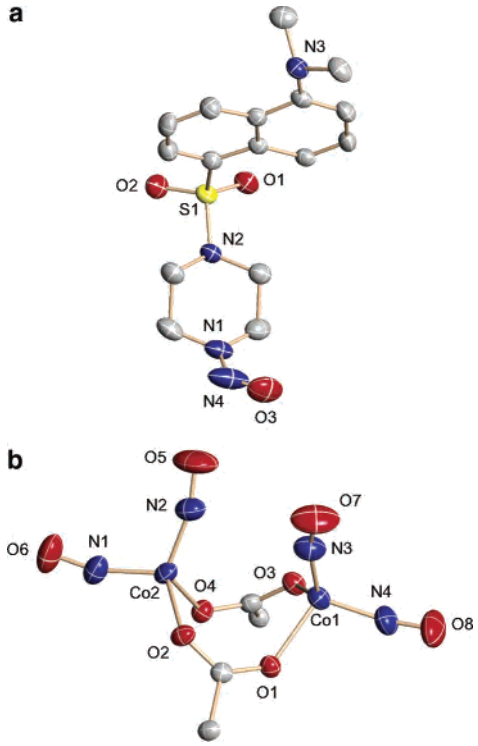

Figure 5. ORTEP diagrams of (a) *N*-nitroso-dansyl-piperazine (**4**) and (b) $[Co_2(NO)_2(\mu\text{-}O_2CAr^{Tol})_2]$ (**5**) showing 50% probability thermal ellipsoids. Only one of the two positions for the disordered oxygen atom (O3) is depicted in (a). The *m*-tolyl terphenylcarboxylate ligands of **5** have been truncated, and the solvent molecule has been omitted for clarity.

ring in **4** are no longer equivalent, as expected after functionalization of the secondary amine to form the *N*-nitroso species. The *N*-nitroso product **4** is moderately air-stable, decomposing only after several days of standing in air.

Concentration of the brown Et_2O filtrate from the nitrosylation reaction followed by crystallization at −40 °C gave dark brown blocks of **5** in 64% yield. With further manipulation of the remaining mother liquor, it was possible to isolate HO_2CAr^{Tol}. X-ray diffraction studies on the dark brown plates revealed **5** to be a dicobalt tetranitrosyl complex in which two of the carboxylate ligands and both of the dansyl-piperazine moieties from **2** were replaced by nitrosyl ligands. Compound **2** thus undergoes reductive nitrosylation to form **5**, which is composed of two carboxylate-bridged $\{Co(NO)_2\}^{10}$ centers (Scheme 2). The average N−O bond length in **5** is 1.15(1) Å, and the average O−N−Co angle is 163(1)°. These values are consistent with those previously reported in the literature for $\{Co(NO)_2\}^{10}$ species.[32−34] In some examples, $\{Co(NO)_2\}^{10}$ units are formed from Co^{2+} starting complexes, with the metal center providing the needed electron to generate the dinitrosyl species by disproportionation of $[Co^{2+}L_2]$ to give $[Co^{1+}(NO)_2L]$ and $[Co^{3+}L_3]$.[35−37] In the present system, however, no Co^{3+} species was isolated. It appears that NO acts as the electron source for reduction of Co^{2+}. The NO^+ equivalent, generated by initial reduction of

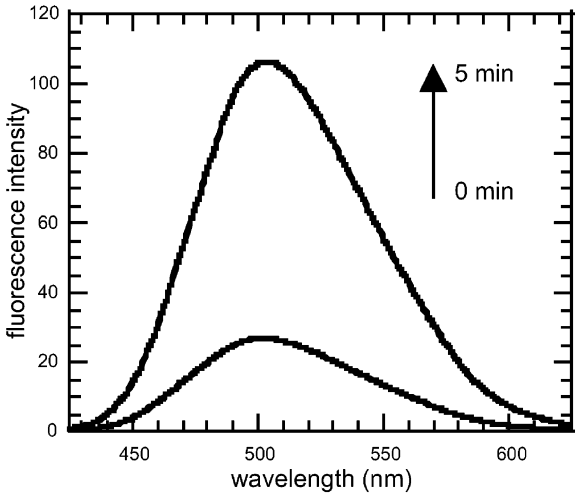

Figure 6. The fluorescence response of a 1×10^{-4} M solution of **1** in CH_2Cl_2 5 min after addition of 1 equiv of NO. Excitation is at 350 nm.

the Co^{2+}, would then be free to react with Ds-pip, forming **4** with concomitant abstraction of the NH proton by the terphenylcarboxylate anion. NO has previously been proposed to be a source of reducing equivalents for the conversion of Fe^{3+} dithiocarbamates to produce Fe^{2+} dithiocarbamate complexes.[38,39] A similar mechanism may occur with the present dicobalt system.

From the X-ray analysis of the products and the solution IR data on the reaction, a possible mechanism can be proposed (Scheme 2). Reaction of NO with **2** may result in formation of an initial mononitrosyl cobalt fragment. Because no such species is observed by solution IR spectral studies, even when conducted at −78 °C, such a species, if present, must be transient and highly reactive. It could then act as an NO^+ source following rapid reduction of the cobalt center to Co(I), which would then be free to consume additional equivalents of NO to generate **5**. The secondary nitrogen atom of the Ds-pip ligand, which may be in close proximity to the putative NO^+ equivalent, would undergo *N*-nitrosation. The presence of a base, such as the *m*-tolyl terphenylcarboxylate anion, could assist by abstracting the amine proton, thereby facilitating formation of **4** and generating an equivalent of HOC_2Ar^{Tol}. The formation of **4** and HOC_2Ar^{Tol} would result in their dissociation from the dicobalt core.

Fluorescence Studies. The reactivity of **1** with NO was investigated by fluorescence spectroscopy. Exposure of **1** to 1 equiv of NO in CH_2Cl_2 results in a 4-fold increase in fluorescence emission intensity within 5 min upon excitation at 350 nm (Figure 6). This fluorescence response, coupled with the solution IR data, indicates significant changes in the diiron core, such as dissociation of Ds-pip. The free ligand, effectively removed from the influence of the iron centers, is the probable source of the increase in fluorescence

(32) Aresta, M.; Ballivet-Tkatchenko, D.; Bonnet, M. C.; Faure, R.; Loiseleur, H. *J. Am. Chem. Soc.* **1985**, *107*, 2994−2995.
(33) Kaduk, J. A.; Ibers, J. A. *Inorg. Chem.* **1977**, *16*, 3283−3287.
(34) Roustan, J.-L.; Ansari, N.; Le Page, Y.; Charland, J.-P. *Can. J. Chem.* **1992**, *70*, 1650−1657.
(35) Del Zotto, A.; Mezzetti, A.; Rigo, P. *Inorg. Chim. Acta* **1990**, *171*, 61−69.
(36) Hendrickson, A. R.; Ho, R. K. Y.; Martin, R. L. *Inorg. Chem.* **1974**, *13*, 1279−1281.
(37) Martin, R. L.; Taylor, D. *Inorg. Chem.* **1976**, *15*, 2970−2976.
(38) Katayama, Y.; Soh, N.; Maeda, M. *Bull. Chem. Soc. Jpn.* **2002**, *75*, 1681−1691.
(39) Fujii, S.; Yoshimura, T.; Kamada, H. *Chem. Lett.* **1996**, 785−786.

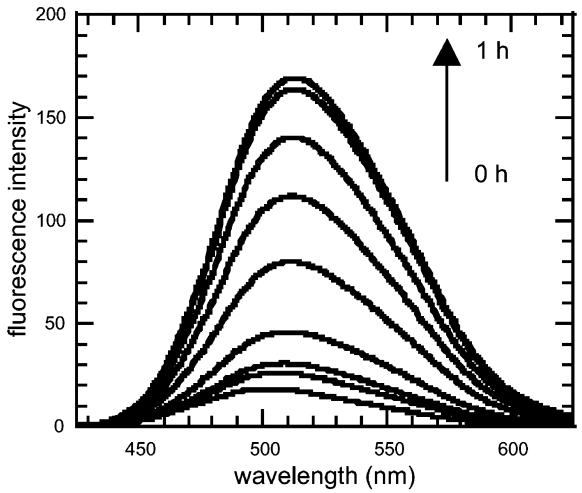

Figure 7. The fluorescence response of a 1×10^{-4} M solution of **2** after admission of excess NO. Traces display the time dependence of the fluorescence response with excitation at 350 nm. Individual spectra are recorded at 0, 1, 5, 10, 20, 30, 40, 50, and 60 min.

emission intensity. In addition to an NO-induced fluorescence response, **1** also reacts with O_2 to afford an increase in fluorescence intensity. When **1** is exposed to 1 equiv of O_2 in CH_2Cl_2, the fluorescence increases slowly by 2.8-fold after 15 min and maximizes at 5-fold after standing overnight (Figure S1, Supporting Information). Although this system fluoresces upon exposure to O_2, its response to NO is significantly faster than for the previously investigated aminotroponiminate compounds.[2] Thus, **1** could serve as an irreversible NO sensor for applications in which its reaction with O_2, a common property of iron(II) aminocarboxylate complexes,[40] is not an issue.

From the X-ray crystallographic results showing dissociation of the dansyl moiety from the cobalt centers when **2** is exposed to excess NO, it is not surprising that an increase in fluorescence intensity is also observed. When **5** is allowed to react with 150 equiv of NO in CH_2Cl_2, a 9.6-fold increase in fluorescence is observed after 60 min (Figure 7). During this period, the emission maximum also shifts from 503 to 513 nm. This shift in emission wavelength is due to *N*-nitrosation of the dansyl-piperazine ligand. When the fluorescence experiment is repeated with 1 or 20 equiv of NO, only 1.2- and 1.4-fold increases in fluorescence intensity, respectively, are observed. The lack of a major fluorescence response with these amounts of NO is consistent with the observed solution IR studies, where the nitrosyl bands and concomitant formation of a brown solution only occurred in the presence of a large excess of NO. The lack of response to small amounts of NO indicates that formation of the proposed initial mononitrosyl intermediate is the rate-limiting step in the reaction and that its formation is only favored in the presence of a large excess of NO. Although air-stable, the low sensitivity and lack of water solubility of this system make it less than ideal for use as a biological NO sensor. If the water solubility could be improved, however, it would be a potential candidate for future development.

(40) Schneppensieper, T.; Finkler, S.; Czap, A.; van Eldik, R.; Heus, M.; Nieuwenhuizen, P.; Wreesmann, C.; Abma, W. *Eur. J. Inorg. Chem.* **2001**, 491−501.

Conclusions

New carboxylate-bridged dimetallic iron(II) and cobalt(II) complexes with fluorophore-containing ligands coordinated to the metal core have been prepared. Design of the complexes was based on previous research indicating that the reaction of NO with the hydroxylase component of soluble methane monooxygenase and synthetic analogues thereof may result in ligand displacement from its diiron core. Both the diiron and dicobalt complexes react with NO to elicit an increase in fluorescence emission intensity caused by dissociation of the fluorophores. Such decomplexation removes them from the nonradiative decay pathways that quench the emission in the parent complexes. In the case of the dicobalt system, the reaction with NO proceeds by reductive nitrosylation, where the cobalt atoms are formally reduced to Co(I) dinitrosyl units. Isolation and characterization of the nitrosylation reaction products provides insight into a possible mechanism for this reaction. Formation of *N*-nitroso dansyl-piperazine indicates generation of NO^+ or an NO^+ donor during the course of the reaction. Thus, it appears that NO is the ultimate source of the electron used to reduce the dicobalt(II) core in the reaction, forming $[Co_2(\mu\text{-}O_2CAr^{Tol})_2(NO)_4]$. These complexes further demonstrate the value of the ligand dissociation strategy to prepare fluorescence-based sensors for NO that evoke an increase in emission intensity.

Acknowledgment. This work was supported by NSF Grant CHE-0234951. The MIT DCIF NMR spectrometer was funded through NSF Grant CHE-9808061.

Supporting Information Available: Figure S1, depicting the fluorescence response of **1** after exposure to dioxygen, and X-ray crystallographic files (CIF). This material is available free of charge via the Internet at http://pubs.acs.org.

IC049649L